Bootstrap a Statistical Brain Atlas

Mei Chen *meichen@ri.cmu.edu*
Takeo Kanade *tk@ri.cmu.edu*
Dean Pomerleau *deanp@assistware.com*
Robotics Ins., Carnegie Mellon Univ.
Assistware Technology

Abstract

Registration of medical images enable quantitative study of anatomical differences between populations, as well as detection of abnormal variations indicative of pathologies. However inherent anatomical variabilities between individuals and possible pathologies make registration difficult. This paper presents a bootstrap strategy for characterizing non-pathological variations in human brain anatomy, as well its application to achieve accurate 3-D deformable registration.

Inherent anatomical variations are initially extracted by deformably registering training data with an expert-segmented 3-D image, a digital brain atlas. Statistical properties of the density and geometric variations in brain anatomy are extracted and encoded into the atlas to build a statistical atlas. These statistics are then used as prior knowledge to guide the deformation process. A bootstrap loop is formed by registering the statistical atlas to larger training sets as more data becomes available, so as to ensure more robust knowledge extraction, and to achieve more precise registration. Compared to an algorithm with no knowledge guidance, registration using the statistical atlas reduces the overall error by 34%.

1. Motivation

Registration between 3-D images of human bodies enables cross-subject diagnosis and post-treatment analysis. However, due to genetic and life-style factors, there are inherent non-pathological differences in the appearance and location of anatomical structures between individuals. Figure 1 displays cross-sections from T1-weighted magnetic resonance imaging (MRI) volumes of two non-pathological brains. The example structure, corpus callosum, has different intensity, shape, size, and location in these two brains. These variations are characteristic for the particular structure of the individuals. For registration algorithms that assume the same structure should have the same appearance or location in different individuals, these innate variations make accurate inter-subject registration difficult.

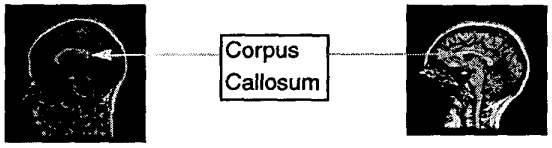

Figure 1. Innate variations between individuals.

Currently there exist many intensity correspondence based registration algorithms [1], [3], [5], [14]. Although they demonstrate encouraging performance, considerable inaccuracies still exist. Certain inaccuracies are caused by the algorithm's insufficient knowledge of the anatomy, and cannot be corrected by exploiting image features solely. Knowledge of anatomical variations will help improve registration performance; furthermore, characterization of such variations can facilitate quantitative study of anatomical differences between populations, as well as anomaly detection.

2. Bootstrap strategy

We intend to capture knowledge of anatomical variabilities in human brain structures, so as to improve inter-subject registration accuracy. The core approach is a closed-loop bootstrap framework for characterizing the appearance of brain structures and their non-pathological variations between individuals, then applying such knowledge to improve registration accuracy, and further using the improved registration to refine knowledge characterization, which helps obtaining more precise registration. This closed-loop bootstrap process can keep going as more image data becomes available, Figure 2 illustrates the concept. In order to extract anatomical variations between individ-

0-7695-0813-8/00 $10.00 © 2000 IEEE

uals, image data of a population needs to be compared in a common reference frame. Our reference is a 3-D digital atlas, which is a T1-weighted MRI of a non-pathological brain, accompanied by expert classification of its anatomical structures. Note that, this atlas is an example of a normal brain, not an average brain of a population. The method for comparison is an automatic 3-D deformable registration algorithm that was previously developed [14].

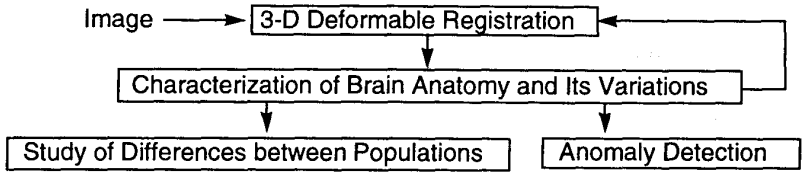

Figure 2. Bootstrap Strategy

3. Capturing anatomical variations

A population of 105 T1-weighted normal brain MRI volumes constitute the training set. Different image acquisition processes result in variations in the 3-D orientation, position, resolution and intensity of image volumes in the training set. Differences in head size also add variation in the scales of the 3-D images. These variations are extrinsic to the anatomical variabilities, and thus need to be removed before the intrinsic variations can be extracted. This is similar to Martin et al.'s approach of separating important and unimportant shape variation so as to quantitatively describe pathological shape variations[8].

3.1. Eliminating extrinsic variations

The registration algorithm employed for atlas-training set comparison [14] consists of a hierarchy of deformable models, of which the first level is a similarity transformation, which addresses the extrinsic geometric variations between different subject volumes via 3-D rotation, scaling, and translation. As a result, each subject volume in the training set has the same orientation, size, and location as that of the atlas. The transformed subject volume is resampled to match the resolution of the atlas. A multi-level intensity equalization scheme is interwoven into the deformation hierarchy to adjust the differences in intensity distributions. The middle row in Figure 3 shows the result of having removed the extrinsic differences between the atlas and samples in the training set.

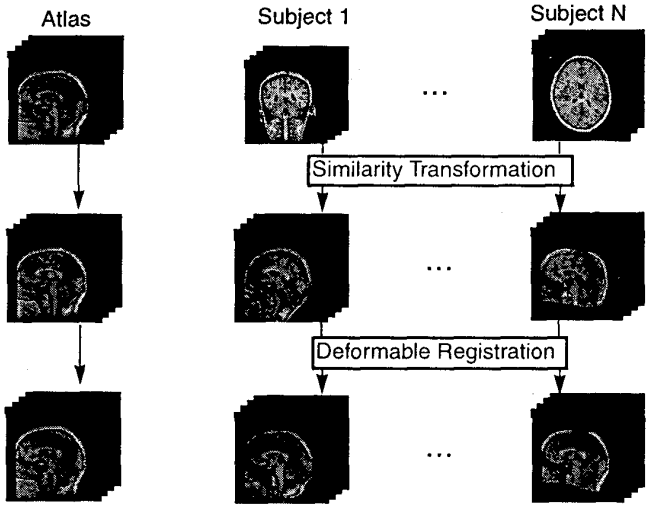

Figure 3. Remove extrinsic variations, and extract intrinsic variations.

3.2. Extracting intrinsic anatomical variations

After the removal of extrinsic variations, intrinsic variations are apparent as the misalignment between anatomical structures in the subject volumes and the atlas. The employed registration algorithm captures this information by aligning corresponding structures through 3-D deformation, as shown in the last row of Figure 3. 3-D displacement at each voxel is recorded. Therefore, after

aligning each subject's anatomical structures with those in the atlas, each atlas voxel is associated with two distributions: one is an intensity distribution of corresponding voxels in the subject volumes; the other is a geometric distribution of the 3-D displacement between the atlas voxel and the corresponding voxels in the subject volumes. The former contains density variations of anatomical structures over a population (density is reflected in image intensity), while the latter embodies geometrical variations such as shape, size, and location.

4. Modeling anatomical variations

The purpose of capturing anatomical variations is to achieve accurate registration. We characterize these variations as statistics, so as to employ them as prior knowledge in statistical models.

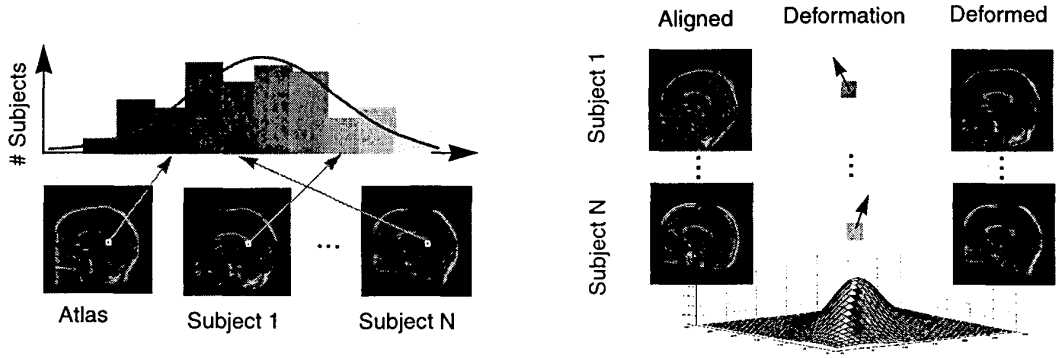

Figure 4. Left: model density variations at each atlas voxel as a 1-D distribution. Right: model geometric variations at each atlas voxel as a 3-D distribution.

4.1. Modeling density variations

Once the training set is deformed to register with the atlas, each atlas voxel corresponds with its counterpart in each of the subject volumes. The histogram of their intensities captures tissue density variations in a population (Figure 4, left).

The intensity histogram at each atlas voxel is modeled as a 1-D Gaussian distribution, $P\langle dI|D\rangle$:

$$P\langle dI|D\rangle = \frac{1}{\sqrt{2\pi}\sigma}\exp\left(-\frac{(dI-\mu)^2}{2\sigma^2}\right) \qquad (1)$$

where $dI = I_s - I_a$, while I_s and I_a are corresponding voxel intensities in the subject volume and the atlas. D is the 3-D deformation between them. μ is the mean intensity difference between the training set and the atlas at this voxel; σ^2 is the variance of the intensity difference distribution. dI has been adjusted for intensity variations caused by image acquisition processes (3.1).

4.2. Modeling geometric variations

After the training set is deformed to register with the atlas, the 3-D displacements between each atlas voxel and its counterparts in the training set embody the geometric variations between individuals. The distribution of the variations can be captured in a 3-D histogram. Figure 4, right, shows a 2-D illustration. The 3-D histogram of displacements at each atlas voxel is modeled as a 3-D Gaussian distribution, $P(D)$:

$$P(D) = \frac{1}{\sqrt{(2\pi)^3|\Phi|}}\exp\left(-\frac{(\overrightarrow{\Delta\vartheta}-\vec{\omega})^T\Phi^{-1}(\overrightarrow{\Delta\vartheta}-\vec{\omega})}{2}\right) \qquad (2)$$

here $\overrightarrow{\Delta\vartheta}$ is the 3-D displacement between the atlas voxel and its counterpart in the subject volume, $\vec{\omega}$ is the mean 3-D displacement at this atlas voxel, and Φ is the 3x3 covariance matrix of the distribution. $\overrightarrow{\Delta\vartheta}$ has been adjusted for extrinsic variations (3.1).

4.3. A statistical atlas

The original atlas was one particular subject's brain MRI data, with each voxel's anatomical classification given by an expert; the above modeling associates each atlas voxel with a distribution of tissue density variations, and a distribution of geometric variations between individuals. These distributions enrich the atlas into a statistical atlas that embodies the knowledge of anatomical variations in a population. Figure 5 illustrates the concept.

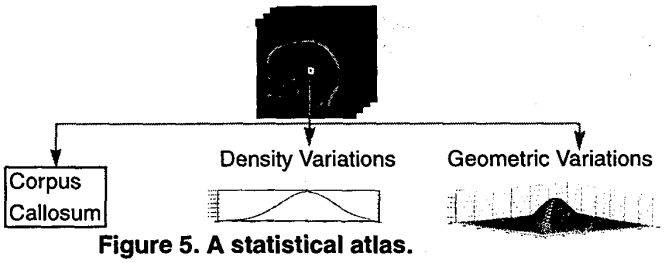

Figure 5. A statistical atlas.

5. Registration using the statistical atlas

Using the statistical models as prior knowledge, the registration between a subject and the atlas can be formulated as finding the deformation D that gives the highest posterior probability $P\langle D|dI\rangle$. According to Bayes rule, $P\langle D|dI\rangle$ can be expressed as:

$$P(D|dI) = \frac{P(dI|D)P(D)}{P(dI)} \tag{3}$$

Finding the highest $P\langle D|dI\rangle$ becomes maximizing the right hand side of equation (3). Here $P(dI)$ is a constant for two given image volumes, and the numerator has the same maximum as its logarithm. Substituting from equations (1) and (2) and taking logarithms, we obtain:

$$\log\frac{1}{\sqrt{2\pi}\sigma} - \frac{(dI-\mu)^2}{2\sigma^2} + \log\frac{1}{\sqrt{(2\pi)^3|\Phi|}} - \frac{(\overrightarrow{\Delta\vartheta}-\overrightarrow{\vartheta})^T\Phi^{-1}(\overrightarrow{\Delta\vartheta}-\overrightarrow{\vartheta})}{2}$$

hence maximizing $P\langle D|dI\rangle$ is equivalent to minimizing the term:

$$\frac{(dI-\mu)^2}{2\sigma^2} + \frac{(\overrightarrow{\Delta\vartheta}-\overrightarrow{\vartheta})^T\Phi^{-1}(\overrightarrow{\Delta\vartheta}-\overrightarrow{\vartheta})}{2} \tag{4}$$

We use gradient descent to find the deformation that minimizes (4). The 3-D gradient, ∇, at each step of the descent is given by the first order derivative of (4):

$$\nabla = \frac{dI-\mu}{\sigma^2}\nabla I + \Phi^{-1}(\overrightarrow{\Delta\vartheta}-\overrightarrow{\vartheta}) \tag{5}$$

where ∇I is the 3-D image gradient, which is a function of the voxel's position. In this way, each voxel is guided to search for a counterpart so their match is most probable according to the statistics gathered from a population. This algorithm differs from the previously developed hierarchical deformable registration algorithm[14] in the measurement of the goodness of the voxel deformation flow. In this method, we maximize the posterior probability of the current deformation using statistics gathered from a population, whereas in the previous algorithm we minimize the intensity difference between spatially corresponding voxels in the atlas and the subject volume. Before undergoing deformation, both algorithms globally align the two image volumes to eliminate extrinsic variations.

Voxel-based statistics models are efficient at modeling anatomical variations. In reality, however, the deformation of neighboring voxels are not independent. A more comprehensive model should consider dependencies between 3-D deformations of neighboring voxels. Theoretically we can address this neighborhood context using a direct higher dimensional extension of the voxel-based statistics models; however, the dimensionality of our image volumes makes this approach impractical for our facility. To simplify the problem, we approximate the voxel-neighbor interaction using the *goodness* of its neighbors' current match according to their respective prior distributions. Using a weighted-window matching approach, the *goodness* is weighted by the distance between the voxel and the particular neighbor. Therefore, for a voxel neighborhood $\Re$, the 3-D gradient determined by neighborhood statistics models is a direct extension of equation (5):

$$\nabla = \sum_{i,j,k} w_{ijk}\left(\frac{dI-\mu}{\sigma^2}\nabla I\right)_{ijk} + \sum_{i,j,k} w_{ijk}[\Phi^{-1}(\overrightarrow{\Delta\vartheta}-\overrightarrow{\vartheta})]_{ijk} \qquad ijk \in \Re$$

6. Performance of registration using the statistical atlas

We start from a small subset of our image data, and bootstrap knowledge characterization till full usage of the training set. The effectiveness of our model of anatomical variations is evaluated by comparing registration using the statistical atlas, and registration using the original atlas.

Since each voxel in the atlas is labelled with the anatomical structure that contains it, when we register the atlas with a subject, we can then assign the label to the corresponding voxel in the subject. This creates a *customized atlas* which contains classifications of the subject's anatomical features. Figure 6, left, illustrates this process. Given the *ground-truth* classification of the subject's anatomical structures, we can evaluate the quality of the registration by assessing the voxel classification accuracy. Currently we have 40 subjects' brain MRIs that have expert classification of one structure, the corpus callosum, in one plane, the mid-sagittal plane. They are not part of the training set, and are used as the test set. Using expert classification as *ground-truth*, we define our error metric as the ratio between the number of mislabelled voxels and the number of expert labelled voxels. Mislabelled voxels include those labelled as corpus callosum in the customized atlas but not by the expert, or vice versa. Note that this ration can be larger than 100%.

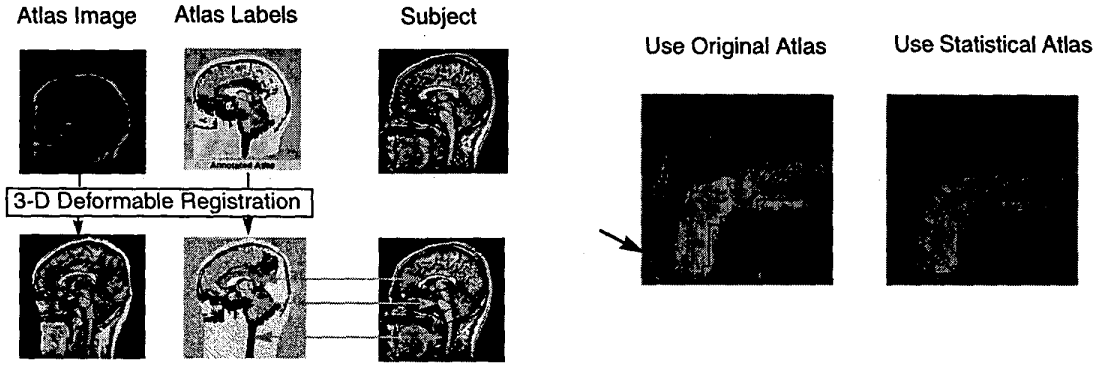

Figure 6. Classifying a subject's anatomical structures through registration with the atlas (left). Registration results using the statistical atlas and the original atlas (right).

When applied to the test set, registration guided by the statistical atlas with a 3x3x3 voxel neighborhood gives an overall mislabelled voxel ratio of 2.9%. This is a 34% error reduction over the algorithm with no knowledge guidance[14]. We expect a complete implementation of the neighborhood statistics guided registration to yield an even greater improvement in performance. Figure 6, right shows an example of improved registration using the statistical atlas.

7. Applications of registration

Accurate and efficient registration algorithms make it possible for quantitative study of the anatomy over large populations. To investigate the feasibility of such approach and its acceptability by medical professionals, several collaborative study have been conducted with research groups in medical institutions.

7.1. Quantitative study of populational differences.

To explore the application of automatic quantitative analysis, segmentation of the right lateral ventricle in 9 schizophrenic patients and 12 normal controls were conducted both by human operators and the registration algorithm (in collaboration with researchers at Western Psychiatric Institute and Clinic of the University of Pittsburgh Medical Center). Histograms of respective volumetric measurements given by both methods are compared in Figure 7, left. The top row shows results given by human operators, with the left histogram for normal controls, and the right one for schizophrenics; the bottom row gives corresponding results from the automatic analysis. Despite a systematic tendency of larger volumes estimated by the automatic algorithm, results from these two methods are highly correlated (Pearson's correlation coefficient = 0.95).

7.2. Detect abnormal variations

Despite drastic individual variability in the anatomy, there still exists a distinction between the normal range of variability and pathology-afflicted alteration. A statistical study of the *skull* volume over a population of 48 normal subjects gives a histogram distribution shown in Figure 7, right. The horizontal axis is the volume of the skull in cm^3, the vertical axis is the percentage of subjects studied. Note the wide range of variations among normal subjects. However, the estimated skull volume in a pathological brain, 106.57 cm^3, still falls beyond the normal range of variations.

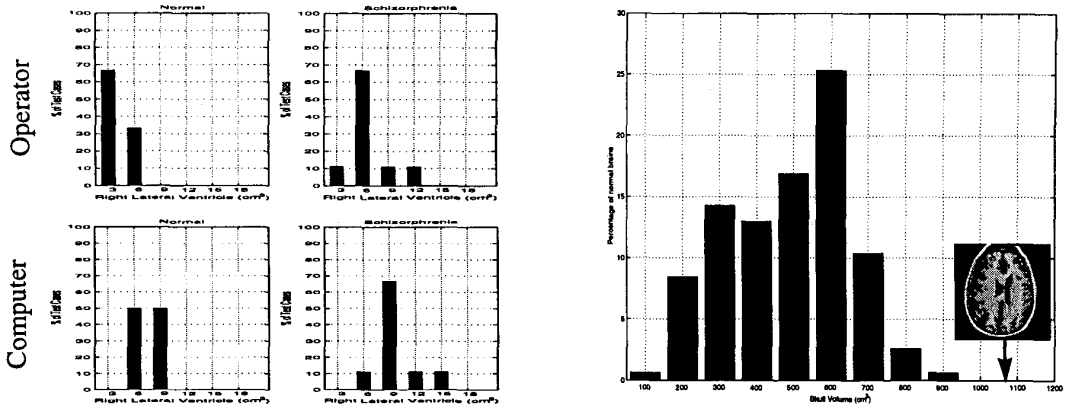

Figure 7. Left: Histograms of right lateral ventricle volumes of normal controls and schizophrenics, from manual estimation (top) and automatic analysis (bottom). High correlation is observed. Right: Histogram of 48 normal subjects' skull volumes. A pathological brain's skull volume falls beyond the normal range of variations

8. Conclusion

Inter-subject registration is made difficult due to inherent differences between individuals. Characterization of such anatomical variations can help improve registration performance. Using a bootstrap strategy, we extract the patterns of variations in the appearances of brain structures from a training set of 105 T1-weighted MRIs. Compared to registration with no prior knowledge, registration using knowledge guidance achieves 34% error reduction on a test set of 40 MRI volumes.

Besides guiding deformable registration, knowledge of anatomical variations can also facilitate quantitative investigation of anatomical differences between populations, and help detect abnormal variations due to pathology.

In the future, one important issue is to refine the statistical atlas by building population-specific atlases. To achieve this, data from large populations need to be stratified into subpopulations. Atlases constructed from subpopulations encode information on population variability, and therefore can facilitate study of identifying group-specific patterns of anatomic or functional alterations.

References

[1] Christensen et al., "Individualizing Neuroanatomical Atlases Using A Massively Parallel Computer", *IEEE Computer*, pp. 32-38, January 1996.

[2] Evans et al., "Warping of Computerized 3D Atlas to Match Brain Image Volumes for Quantitative Neuroanatomical and Functional Analysis. *Proceedings of SPIE Medical Imaging*, vol. 1445, pp. 236-246.

[3] Vemuri et al., "An Efficient Motion Estimator with Applications to Medical Image Registration", *Medical Image Analysis*.

[4] Bajcsy and Kovacic, "Multiresolution Elastic Matching", *Computer Vision, Graphics, and Image Processing*, vol. 46, pp 1-21, 1989.

[5] Jean-Philippe Thirion, "Fast Non-Rigid Matching of 3D Medical Images", INRIA, Technical Report No. 2547, May, 1995.

[6] Szekely et al., "Segmentation of 2-D and 3-D objects from MRI volume data using constrained elastic deformations of flexible Fourier contour and surface models", *Medical Image Analysis*, vol. 1, No. 1, pp. 19-34.

[7] Bookstein, "Landmark methods for forms without landmarks: morphometrics of group differences in outline shape", *Medical Image Analysis*, vol. 1, No. 3, pp. 225-243.

[8] Martin et al., "Characterization of Neuropathological Shape Deformations", *IEEE Transactions on Pattern Analysis and Machine Intelligence*, vol. 20, No. 2, 1998.

[9] Guimond et al., "Automatic Computation of Average Brain Models", *Proceedings of the First International Conference on Medical Image Computing and Computer-Assisted Intervention*, pp. 631-640, 1998.

[10] Wang and Staib, "Elastic Model Based Non-rigid Registration Incorporating Statistical Shape Information", *Proceedings of the First International Conference on Medical Image Computing and Computer-Assisted Intervention*, pp. 1162-1173, 1998.

[11] Thompson et al., "High-Resolution Random Mesh Algorithms for Creating a Probabilistic 3-D Surface Atlas of the Human Brain", *NeuroImage*, vol 3, No. 1, pp. 19-34, February, 1996.

[12] Gee and Le Briquer, "An Empirical Model of Brain Shape", *Maximum Entropy and Bayesian Methods*, August 4-8, 1997.

[13] Joshi et al., "On the Geometry and Shape of Brain Sub-Manifolds", *International Journal of Pattern Recognition and Artificial Intelligence*, vol. 11, No. 8, pp. 1317-1343, 1997.

[14] Mei Chen et al., "Anomaly Detection through Registration", *Pattern Recognition*, vol 32, pp. 113-128, 1999.